RESEARCH PAPER

LARGE-SCALE HYDROMORPHOLOGICAL CHARACTERISTICS OF THE PROGLACIAL RIVER KATUN (OB HEADWATERS)

Friedrich Seidl[1*], Markus Reisenbüchler[1], Peter Rutschmann[1], Liubov V. Yanygina[2], Martin Schletterer[3]
[1]Chair of Hydraulic and Water Resources Engineering, Technical University Munich, Arcisstr. 21, 80333, Munich, Germany
[2]Institute for Water and Environmental Problems SB RAS, Ulitsa Molodezhnaya 1, 656038, Barnaul, Russia
[3]Institute of Hydrobiology and Aquatic Ecosystem Management, University of Natural Resources and Life Sciences, Gregor-Mendel-Straße 33, 1180, Vienna, Austria
***Corresponding author:** friedrich.seidl@tum.de
Received: February 27th, 2022 / Accepted: May 4th, 2023 / Published: July 1st, 2023
https://DOI-10.24057/2071-9388-2022-022

ABSTRACT. During the industrialization in Europe, rivers were straightened and designed to fit human activities, thus nowadays only a few natural river systems remain as reference conditions as well as guiding principles for river restoration projects. Therefore, the natural state of some river types is often described using historic records and maps. This study aims to analyze the key characteristics of a pristine proglacial river Katun in the Altai mountains and contribute to the knowledge about reference conditions. For this purpose, hydromorphological characteristics like slope, sinuosity and river width of the river Katun were analysed and summarized using different GIS techniques. Additionally, pebble counts were carried out to assess the changing sediment composition along the longitudinal continuum. Combined with River Habitat Surveys and a one-dimensional flow simulation using HEC-RAS it was possible to give a holistic overview of the dynamic fluvial system Katun in its upper, middle and lower reaches. The results confirmed the relationship between the river and its surrounding topography as they clearly show the lateral development of the Katun. As shown for the individual parameters (e.g., slope, width, depth, flow velocity, shear stress), they influence each other and are strongly dependent and characteristic for each river section. In the context of revitalisation of straightened and / or channelized river courses, it is important to focus on the processes of this interaction and provide suitable space for lateral expansion. The study can be seen as a recommendation on how to analyse hydromorphological characteristics of fluvial systems as well as to establish guiding principles in river restoration using remote sensing.

KEYWORDS: hydromorphology, ecohydraulics, proglacial river, Katun, Altai Mountains, Russia

CITATION: Seidl F., Reisenbüchler M., Rutschmann P., Yanygina L. V., Schletterer M. (2023). Large-Scale Hydromorphological Characteristics Of The Proglacial River Katun (Ob Headwaters). Geography, Environment, Sustainability, 2(16), 110-120
https://DOI-10.24057/2071-9388-2022-022

ACKNOWLEDGEMENTS: We acknowledge the „Verein Freunde des Lehrstuhls für Wasserbau und Wasserwirtschaft der Technischen Universität München e.V.", which provided financial support to the excursion in 2019.

Conflict of interests: The authors reported no potential conflict of interest.

INTRODUCTION

The European Directive 2000/60/EC established a framework for community action in the field of water policy in the European Union. It is based on the consideration that water is not a common commercial commodity, but rather an inherited asset that must be protected, defended and preserved[1]. This Water Framework Directive (WFD) aims to harmonise the water policies of all European Member States in order to achieve the best possible protection and the greatest possible restoration of the ecological quality of running waters[1]. Essentially, this balancing act between a Europe-wide standard of protection and the consideration of local particularities is to be achieved through a uniform procedure within the framework of the assessment and classification of water bodies.

The typification and standardisation required in the individual steps subsequently demanded a new, holistic approach to river characterisation and its aquatic habitats[2] and, in particular, included hydromorphology in the assessment of European watercourses (Newson and Large 2006). With the implementation of the WFD not only definitions and study objectives changed, but also a variety of new methods for the analysis and assessment of watercourses with regard to the new aspects were developed (Belletti et al. 2015). However, no common

[1]European Parliament (2000). Directive 2000/60/EC of the European Parliament and of the Council of 23 October 2000 establishing a framework for Community action in the field of water policy. OJ L 327, 22.12.2000, p. 1–73.
[2]European Standard BS EN 14614:2004 (2005). Water Quality [Accessed 08. Oct. 2019].

procedure for hydromorphological surveys of streams and rivers was developed.

The CEN[3] standard from 2002 provides an overview of the most widely accepted characteristics in the context of hydromorphological surveys. In order to determine hydromorphological reference conditions for European rivers, it is often necessary to look beyond the borders of Europe, where the industrialisation resulted in numerous heavily modified river systems and only a few rivers remained in pristine condition (Zerbe 2019).

Accordingly, this work aims to explore the possibility to derive typical hydromorphological aspects of pristine rivers by GIS-based methods in combination with one-dimensional flow simulation, using the Russian proglacial river Katun as a case study. As many rivers in Europe are affected by hydromorphological changes due to land use and flood protection, the data set from Katun can be used as guiding principal for restoration projects at similar rivers in the Alps.

STUDY AREA

The Katun River is considered to be a river system in near-natural condition, due to the low density of settlements and low industry. Thus, this river can develop and shape its course to its full extent of the dynamic processes (Mandych 2006). The biggest spatial limitations are natural characteristics, e.g., narrow gorges and terraces. Therefore, the Katun catchment forms a unique reference catchment to study large-scale hydromorphological characteristics of proglacial rivers and can make a huge contribution towards establishing guiding principles when restoring these rivers in the alpine region.

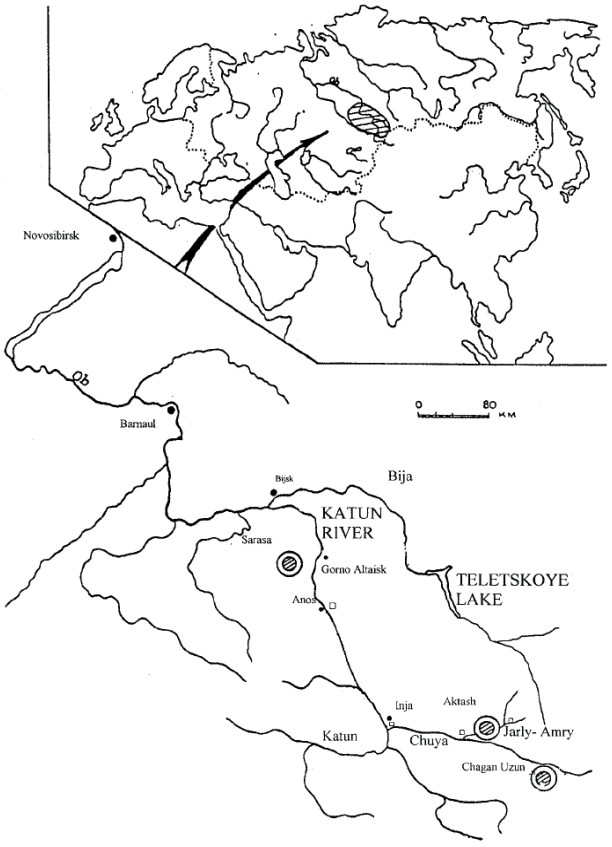

Fig. 1. Location of the Katun river in the Russian Altai Mountains (from: Baeyens et al. 2003)

The Katun River originates from the Gebler Glacier on the Belucha mountain at an elevation of 2640 m a.s.l.[4] in the Russian Altai (Haywood 2010). Along its course towards the north it covers a catchment area of about 60,900 km^2 until it reaches the village of Odintsovka at an altitude of about 200 m above sea level[4]. Downstream of the city of Biysk, after a length of 688 km it joins the river Biya (Mandych 2006; Schletterer et al. 2021a). From the junction of the two rivers the Ob is formed, which flows into the Kara Sea in the north of Siberia. On its way to the Arctic Ocean, the Ob covers a flow distance of 3650 km, making it one of the largest river systems in the world with a catchment area of 2,972,497 km^2 and a MQ near the mouth at Salekhard of 12,600 m^3/s (Shiklomanov et al. 2006). As the longest headwater river, the Katun has an important influence on the Ob River. The mean flow (MQ) of the Katun comprises about 600 m^3/s at the gauge Srostky at river km 616. The Katun is divided into upper, middle and lower reaches based on its tributaries and characteristics. The orographically left tributary Koksa near the town of Ust-Koksa at river kilometer 210 represents the border between the Upper and Middle Katun. The middle course extends to river kilometer 410, where the Sumulta River joins the Katun on the orographic right. The lower course extends from Sumulta River to the confluence with the Biya where both rivers from the Ob near the town of Biysk (Sapozhnikov 1949; Schmalfuß et al. 2022). The flow regime of the Katun can be described according to FOEN (2013) as glacio-nival. Records show an annual fluctuation in discharge typical for this flow regime, with an annual peak discharge as a result of snow and glacier melt. Based on the 1952 glacier area (749 km^2), the Katun River basin has a degree of glaciation of approximately 1% (in the upper course 1.3 %, in the middle course 2.5 % and in the lower course 0 %) (Revyakin 1978). In 1952, the glacier area of the Upper Katun was 173.3 km^2, the Middle Katun (Argut and Chuya basins) – 575.9 km^2 (Khromova et al. 2021). By 2019, the glacier area decreased by about 30% (523 km^2)[5]. Less than 20 % of the runoff is contributed by precipitation and almost 30 % comes from groundwater. The remaining 50% is made up from meltwater of snowfields or seasonal snowfall as well as meltwater from glaciers (Mandych 2006).

MATERIALS AND METHODS

Along the Katun three gauging stations are located, with freely accessible data measuring only the discharge and precipitation starting in 1938 up to the year 2000 (Fig 2). Representative months for low (February), medium (April/September) and high discharges (June) were selected from discharge curves of three different discharge stations at the Katun (Fig. 2).

The hydromorphological analyses of Katun river were carried out with GIS-based data material. The satellite data from Table 1 used in this work were obtained from the freely accessible online portals EarthData of NASA[6] and EarthExplorer of the U.S. Geological Survey[7]. To generate an equal starting point for further selecting the best

[3]CEN (2002). A guidance standard for assessing hydromorphological features of rivers. CEN TC 230/WG2/TG 5 N32, 21 pp.
[4]Esri (2013). "Topographic" [base map]. Scale Not specified. "World Topographic Map." Available at https://services.arcgisonline.com/ArcGIS/rest/services/World_Topo_Map/MapServer [Accessed 31. Oct. 2019]
[5]https://www.glacrus.ru/ледниковые-районы/алтай
[6]https://earthdata.nasa.gov/
[7]https://earthexplorer.usgs.gov/

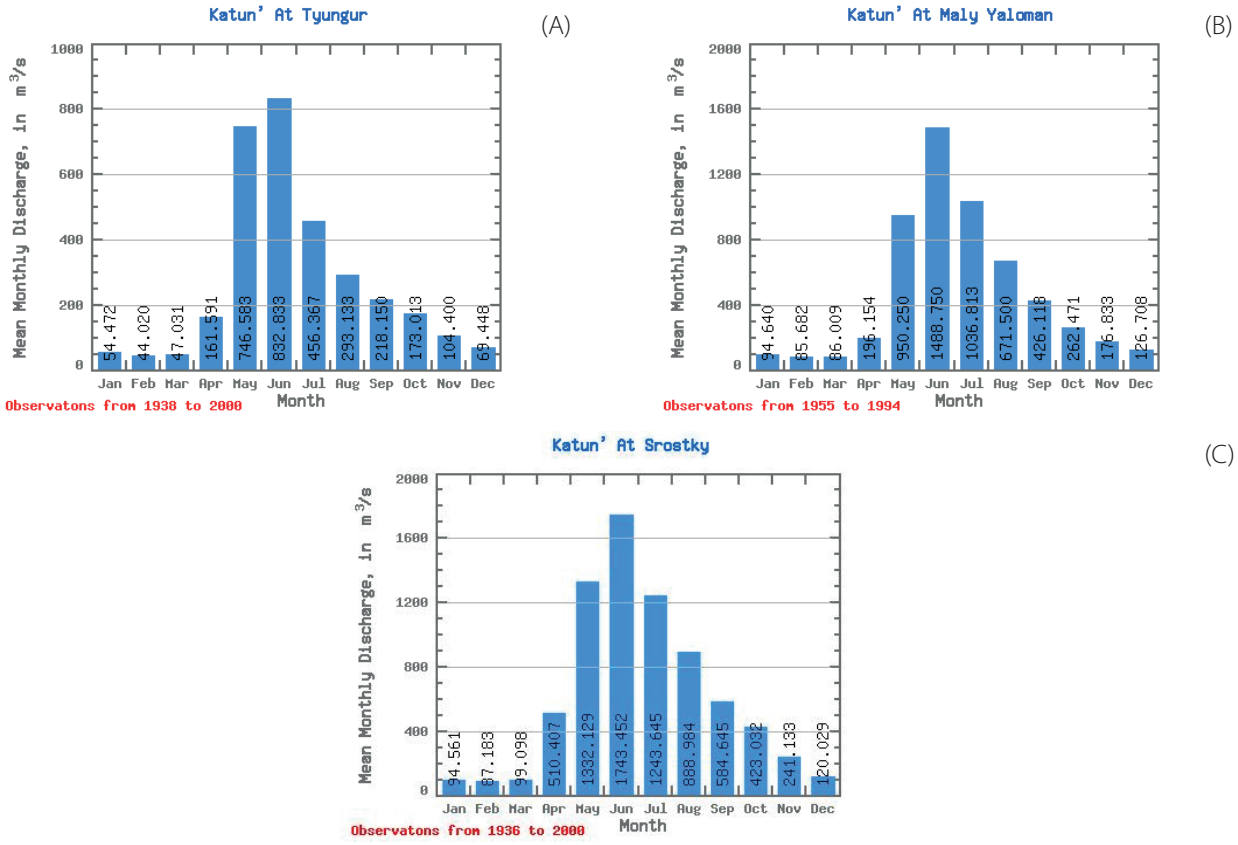

Fig. 2. Averaged monthly discharge of the Katun River in the period 1936 to 2000 at three different stations (from: Lammers et al. 2016)

fit DEM for the performed analysis, the river networks with corresponding flow order were calculated on every available DEM. Afterwards the channel of the River Katun with its most important tributary Chuya were isolated. Since fluvial ecosystems exhibit a distinct hierarchical order in nature (Allan and Castillo 2007) the derived channel was categorized based on stream order (Strahler 1957) to create distinct reference points for the evaluation of the following research. Continuing from there the data was used to extract the sinuosity, width variability and slope of the Katun as follows.

Sinuosity

In order to investigate the sinuosity, the river has to be divided into individual sections, for which the sinuosity was be determined. Therefore, to recommend an appropriate size for the sections on a river length of about 688 km, this work resorted in the first step to a simplified definition of sinuosity (Haggett und Chorley 1969), which was applied to three different section lengths (1 km, 5 km and 10 km):

$$Sinuosity = \frac{length\ of\ river\ axis}{Linear\ distance\ between\ section\ starting\ and\ end\ point} \quad (1)$$

Based on these results the second step was to identify distinctive points along the Katun for which more detailed analyses according to Mueller`s sinuosity index (Mueller 1968) were carried out (Fig. 3). The detailed calculations focused on the Hydraulic, Topographic and Standard Sinuosity Index (HSI, TSI and SSI), as well as again different river section sizes (5, 25 and 50 km) for which the three indices were considered. In addition, when selecting the

$$Channel\ Index\ CI = CL/AL \quad (2)$$

$$Valley\ Index\ VI = VL/AL \quad (3)$$

$$HSI = (CI - VI)/(CI - 1) \quad (4)$$

$$CL = Channel\ Length$$

$$TSI = (VI - 1)/(CI - 1) \quad (5)$$

$$VL = Valley\ Length$$

$$SSI = CL/VL \quad (6)$$

$$AL = Air\ Length$$

Table 1. Available Digital Elevation Models for the Study Area

DEM	Source	Temporal Cover	Resolution
GTOPO30	(USGS 1996)	1993 – 1996	30 Arc Second = 1km
GMTED2010	(USGS 2011)	Nov 2010	7.5 Arc Second = 225m
SRTM VoidFill	(USGS 2012)	Feb 2000	3 Arc Second = 90m
SRTM Global	(USGS 2014)	Feb 2000	1 Arc Second = 30m
ASTER v3.0	(NASA et al. 2001)	2000 – 2013	1 Arc Second = 30m

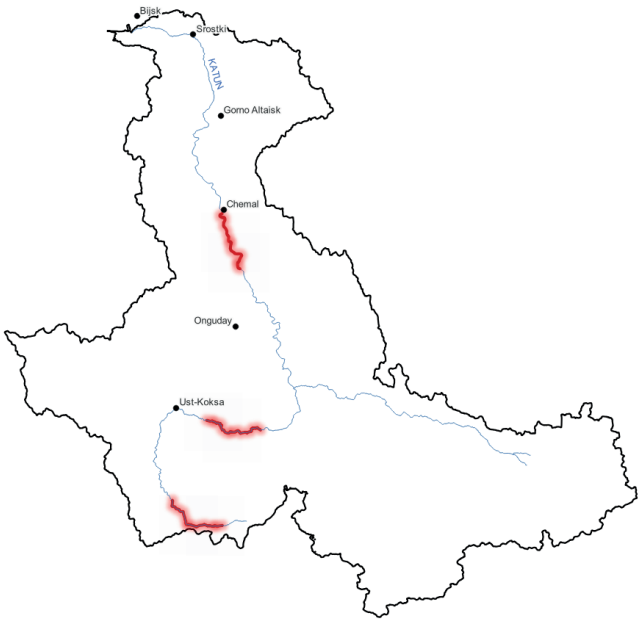

Fig. 3. Locations at the Katun selected for detailed sinuosity calculations

sections, care was taken to avoid settlements on the banks of the Katun, since bank obstructions must be assumed there (Khan et al. 2018).

River Width

The relationship between river width and discharge along the course of a river is one of the most constant relationships among hydraulic variables in natural rivers (Leopold and Miller 1956) and must be considered when analysing the river width using GIS-based data. Herein, the open-access database "Global River Widths from Landsat - GRWL" (Allen and Pavelsky 2018) was used to illustrate the overall tendencies of the river width based on the average discharge along the Katun from its source to its confluence with the Biya River. To analyse interannual variations due to fluctuations in discharge, the river-width was additionally detected from freely available Level 2 Landsat 8 data[8] using the Normalized Difference Water Index (NDWI) and the program ArcGIS[9,10]. The NDWI was calculated as follows (Du et al. 2016):

$$NDWI = (Green - NIR) / (Green + NIR) \quad (7)$$

The Landsat Imagery was gathered for the initially defined months with characteristic discharges based on Fig. 2. Due to the snow cover during winter months in the Altai Mountains, no usable Landsat data for low discharge months could be gathered. Based on the dimensions of the Katun, four hydromorphological characteristic sections with a length between 20 and 30 km were selected. One section each for the upper and middle reaches and due to the different characteristics of the upper and lower sections of the lower reach, two sections were selected for the latter. For the Chuya tributary, a short section just before the confluence with the Katun was considered additionally.

Slope

The determination of the river bottom slope was based on the digital terrain models used and the river axes calculated from them. However, it is not possible for satellites to measure the actual river bottom since the radiation is reflected at the water surface - the values of the DEM therefore correspond to the height of the water surface. While other researchers have already acknowledged this problem and looked into possible solutions (Dai et al. 2018; Purinton and Bookhagen 2017), for simplification, the slope of the water surface was equated with the bottom slope in this work under the assumption of laminar flow. In order to represent the elevation profile of the Katun in longitudinal section, individual points were generated at intervals of one kilometer along the river axes at which the raster values based on the DTMs GTOPO30, SRTM Global and GMTED2010 were extracted. The decisive factor for the choice of this distance was the resolution of the DTM GTOPO30 of 1 km. Even though a higher data density could be chosen for SRTM Global with a resolution of 30 m, this was not done in favour of comparability. At these points, the raster values of the respective terrain model were extracted. The bed slope was then derived from the elevation differences of the individual points.

Stream structure survey and Pebble Count

Additionally, a hydromorphological survey based on the River Habitat Survey (Environment Agency 2003) adapted to the circumstances was conducted by the author along the Katun River during an excursion in September of 2019 (Schletterer et al. 2021b). Surveys were carried out in the middle and lower reaches, including bedload characterisation with *Wolman-Counts* (Wolman 1954; Nikora et al. 1998; Galia et al. 2017) along the banks (Fig. 4). Limitations of this method, besides the lack of detection of fine sediments, are difficulties of measurement at large water depths and the difficult comparability with sieve curves, since the counting methodology provides a cumulative curve based on the total number and not the weight of the sample. Due to the dimensions of the Katun, measurements along the river bottom in a cross section had to be omitted in this work and the lines were measured near the banks on representative gravel bars. At least three lines were measured at each location. To ensure a sufficient amount of data, a sample size of about 150 stones per line was used in this work. The measured stones were divided into twelve different grain fraction classes ranging from grain sizes smaller than 8 mm up to over 256 mm (Table 2).

One-dimensional Model using HEC RAS

The collected data of the above-mentioned analysis was combined into a one-dimensional steady-state flow simulation using HEC RAS 5.0.7 and HEC GeoRAS 10.5 with the aim of connecting parameters observed via GIS-based methods and the rivers hydraulic processes. The values of the three available discharge stations served as authoritative input parameters for the extension of the one-dimensional flow model of the Katun. No discharge values were available for the Upper Katun thus the Tyungur (upstream) and

[8]EROS (2014). Collection-1 Landsat OLI Level-2 Surface Reflectance (SR) Science Product. Ed. by Earth Resources Observation And Science (EROS) Center.
[9]Dilts, T. E. (2015). Polygon to Centerline for ArcGIS: University of Nevada Reno. Available at: https://www.arcgis.com/home/item.html?id=bc642731870740aabf48134f90aa6165 [Accessed 31. Oct. 2019].
[10]Singh, J. (2017). Calculate Road/Stream widths. Available at: https://www.arcgis.com/home/item.html?id=ede4729410e846638520f99901542518 [Accessed 31. Oct. 2019].

Table 2. Grain fraction classes used in pebble count

Grain fraction class	1	2	3	4	5	6	7	8	9	10	11	12
Diameter [mm]	<8	8-11.3	11.3-16	16-22.6	22.6-32	32-45	45-64	64-90.5	90.5-128	128-181	181-256	>256

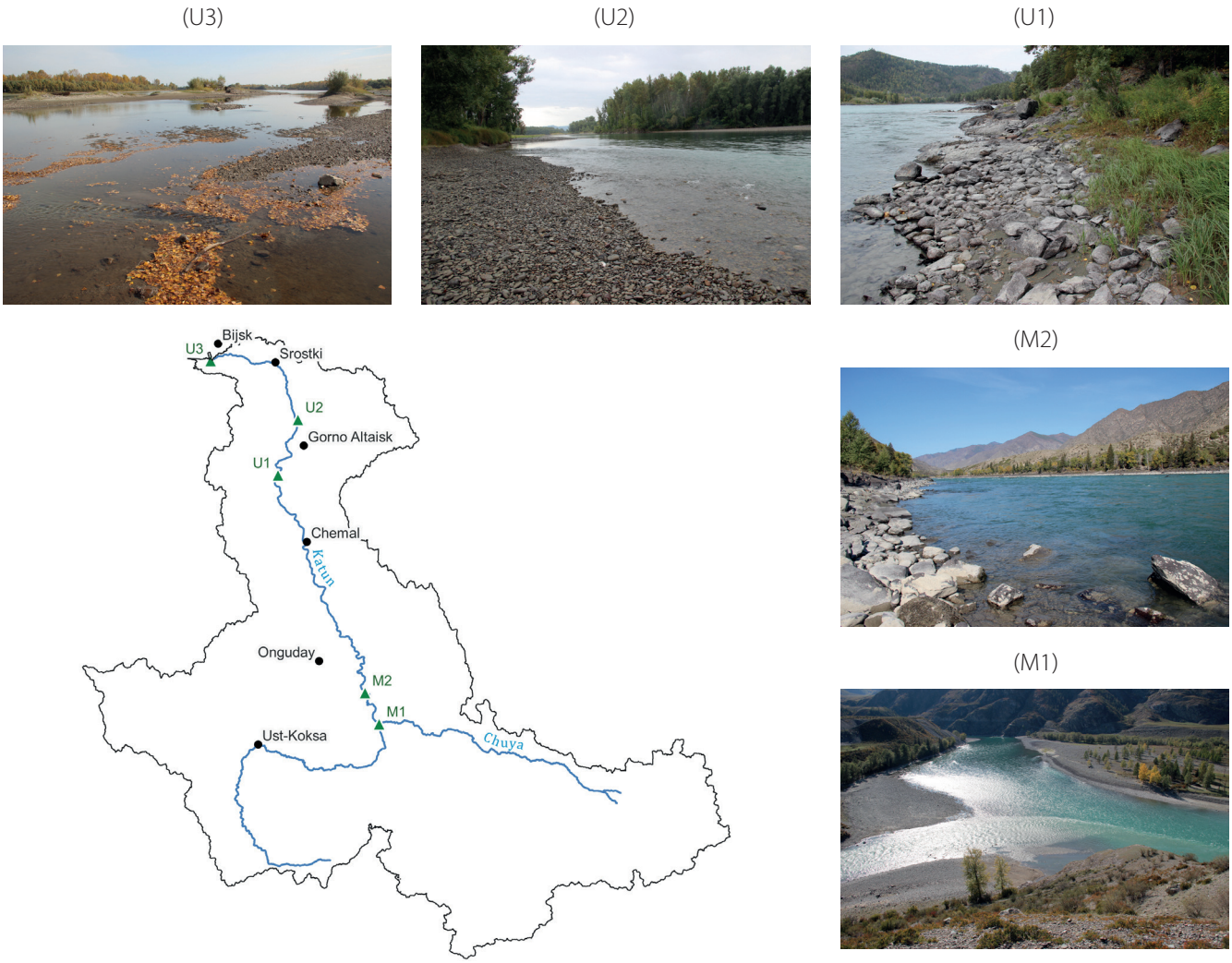

Fig. 4. Locations of stream structure surveys and pebble counts along the Katun

Srostky (downstream) stations were chosen as the start and end points of the model. This resulted in a total length of nearly 370 km, covering large portions of the Lower and Middle Katun as seen in Fig. 5. As clearly seen in the discharge, the lowest flows occur in winter and the highest ones are related to snow and glacier melt (May – July). Based on the collected discharge data from (Lammers et al. 2016), the fluctuations and long-term trends during these months were examined. Due to missing data for the Maly Yaloman station in the middle of the river section and taking into account that an adjustment of the average values under the aspect of the observed strong annual fluctuations was being considered error-prone, for the later simulations average discharge values as seen in Fig. 2 were taken (Table 3).

The remaining parameters of the model were derived from the geoinformation-based calculations already performed (geometries, slopes, river axis, etc.). Since no grain distribution of the actual riverbed could be gathered and the Manning values from the pebble count differed from the literature, the values of the recommendations from literature (Chow 1959; Brunner 2016; Arcement and Schneider 1989) were used in this work for the one-dimensional flow model as shown in Table 4. The ice thickness during the winter months with its associated roughness were determined from literature (Vuglinsky and Valatin 2018). According to Shiklomanov and Lammers (2014) and the available Landsat 8 imagery from the month of April 2019, the end of river glaciation was determined between March and April.

The Strickler Coefficient was derived using the correlation between grain size and bed roughness by inverting the calculated Manning value.

$$n = 0.034 * d^{1/6} \quad (8)$$

RESULTS AND DISCUSSION

The Katun in its upper reaches can be defined as a fourth to fifth order river. With the mouth of the Koksa, the Katun changes to sixth order. This also marks the border between the upper and middle reach in the literature. The inflow of the Chuya increases the stream order to seven. Even though the Chuya is one of the longest tributaries of the Katun (Mandych 2006), the conjunction of both rivers does not lead to a significant change in the river regime and therefore, the lower reach begins where the Sumulta River joins the Katun. Until its confluence with the Biya River, the Katun remains a seventh-order river.

The longitudinal zonation is characteristic for fluvial systems, which is associated with characteristic hydromorphology and bedload processes (Schumm 1977; Allan and Castillo 2007). Our satellite-based investigations

Table 3. Average discharge in the months of February, April, June and September

Station (river km)	February [m³/s]	April [m³/s]	June [m³/s]	September [m³/s]
Tyungur (229)	44	161	832	218
Maly Yaloman (301)	85	196	1488	426
Srostky (616)	87	510	1743	584

Table 4. Manning`s roughness values used in the one-dimensional modelling

River section	Left bank	Main channel	Right bank
Lower Katun	In winter: 0.070 In summer: 0.100	0.035	In winter: 0.070 In summer: 0.100
Medium Katun	0.05	0.04	0.05

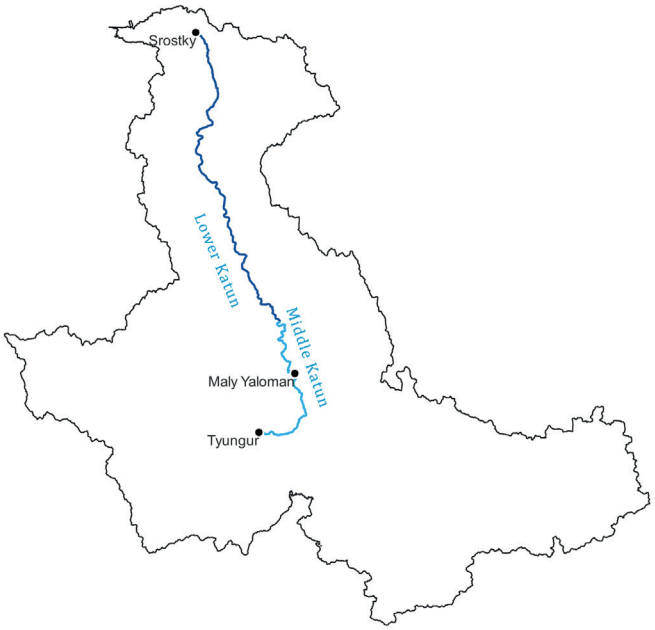

Fig. 5. River section used for one-dimensional flow simulation in HEC RAS

of the Katun River, support the published longitudinal zonation (upper, middle, lower reaches). The elevation profile shows in the linear approximation a slope ranging from 0.29 % to 0.59 % in the upper course. With increasing flow distance it drops to 0.18 % in the middle course and finally to 0.12 % in the lower course (Fig. 6). The results showed that a development of the bed slope and a possible bed deepening in the comparison of the considered years could not be represented justifiably due to the different resolution of the DEMs. Especially in the gorges of the Upper and Middle Katun, the elevation values of the DEMs with resolution ranges of 1 km and 225 m, respectively, often did not represent the water surface, but predominantly that of the adjacent slopes. Therefore, only the results of the observation of the SRTM Global with a resolution of 30 m were deemed accurate.

The different river sections are also clearly visible in the one-dimensional modelling of three different discharges using HEC-RAS. Both the shear stresses and the flow energy in the Middle Katun are a multiple of those in the Lower Katun. This is true both in winter, when the lowest discharge prevails and the river is frozen, with a shear stress of 20 N/m² to 9 N/m² and energy of 41 N/ms to 14 N/ms, and in early summer during the annual flood, with 100 N/m² to 14 N/m² and 404 N/ms to 178 N/ms (Fig. 7).

This energy gradient along the Katun River can be reassured in both the pebble count (Fig. 8) and the visual assessments of the stream structure survey conducted along the river banks. The giant bars and large boulders (Iturrizaga 2011) that shape the riverbed in the middle reaches (M1-M2) and upper lower reaches disappear once the river reaches the flat plains (U1-U3). Here it begins to meander and the predominant grain size is below 32 mm.

In addition, the widening and slowing down of the river can be seen in the simulated water depths but also in the flow velocities (Fig. 9.). The discharge data from the Katun River (Fig. 2) shows that, the volume of the flow increases with increasing flow length due to a larger catchment area caused by numerous tributaries. Within the HEC RAS simulation, the occurring velocities in the lower reaches (max. 2.36 m/s) are noticeably lower than in the middle reaches (max. 2.74 m/s). Considering the slope of the riverbed, this is an understandable relationship. If we now take the average water depths of 3.74 m in the lower reaches to 4.88 m in the middle reaches from Fig. 9 into account, the flow profile in the considered section of the lower reaches must increase, in order to accommodate the increased discharge of approximately 250 m³/s with decreasing velocities and depths. Consequently, as the flow depth decreases, an expansion in width takes place. The maximum river widths in the middle reaches range between 300 m and 400 m, up to 3,500 m in the lower reaches (Fig. 10). In contrast, in the upper section of the lower reaches, river widths of around 250 m were measured. In this area the Katun runs constricted between mountain slopes and is therefore unable to expand. To cope with the increasing discharge and the reduced width, the flow velocities increase to 1.5 m/s and 4 m/s and maximum flow depths of 2 m to 4.5 m during high discharges. As the river leaves the constricted valley and becomes wider, these values drop to 0.5 m/s to 2.5 m/s and 1 m to 2 m, respectively. The consistency of the results is maintained when annual variations are considered.

The Katun River has characteristic flow fluctuations, i.e., the strongly varying flows, over the year (Fig. 2). The river carries 20 times as much discharge in summer as in winter. The reason for this is heavy snowfall in winter, which, together with the thawing of the river at the end of the winter months, leads to increasing discharges in the following months. Since runoff data for these months are available and with the help of a study of the river ice thickness in the Altai Mountains the required parameters could be estimated, it was possible to simulate the hydraulic quantities also for February. Especially the shear stresses and the flow energy show a slowing down of the river. However, with increasing discharges, these values also increase again and in June/July, the highest erosive activity is to be expected due to the shear stresses. Due

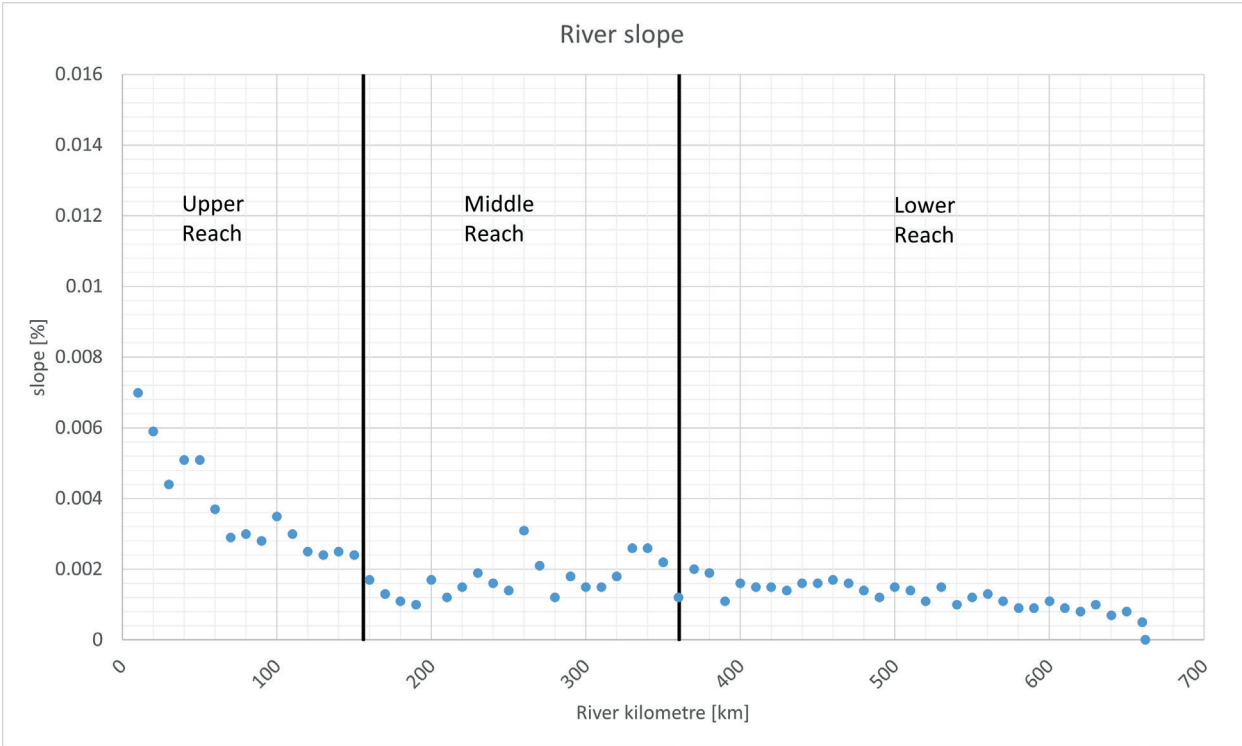

Fig. 6. River slope over 10 km flow segments based on SRTM GLOBAL

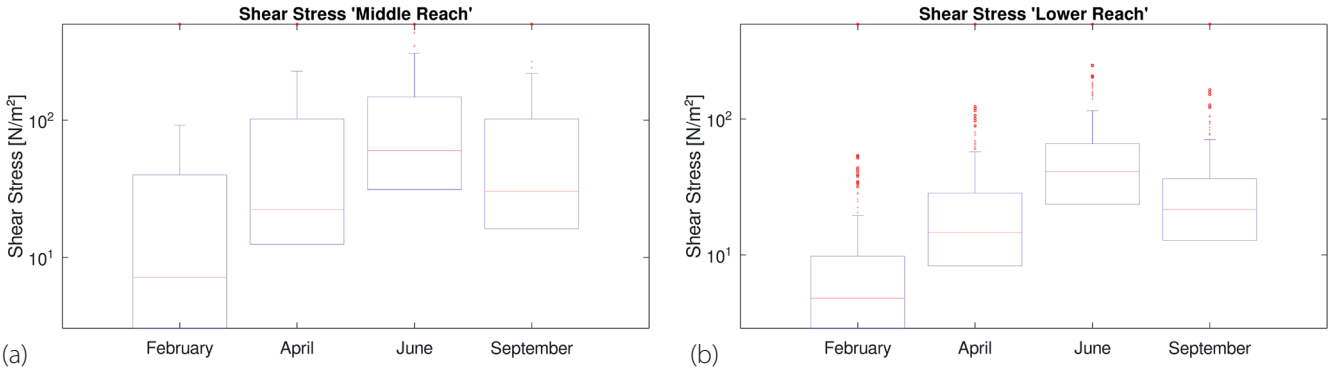

Fig. 7. Annual shear stress variability based on one-dimensional flow simulation in HEC-Ras – a) middle reach b) lower reach

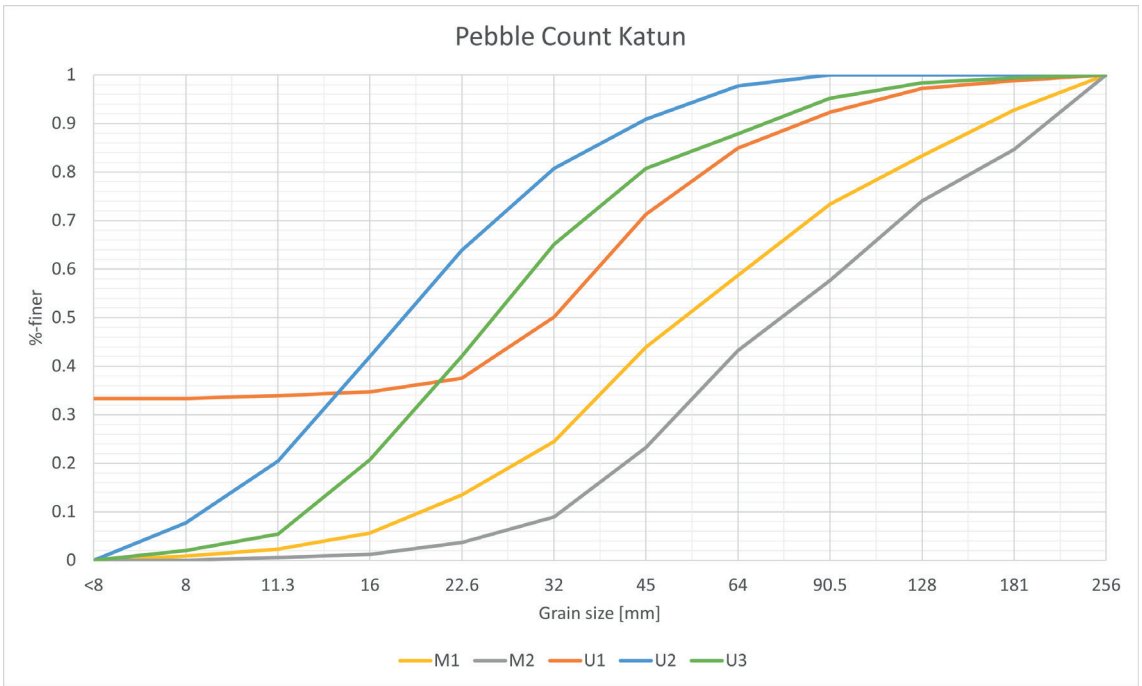

Fig. 8. Sum curve of the pebble count analysis

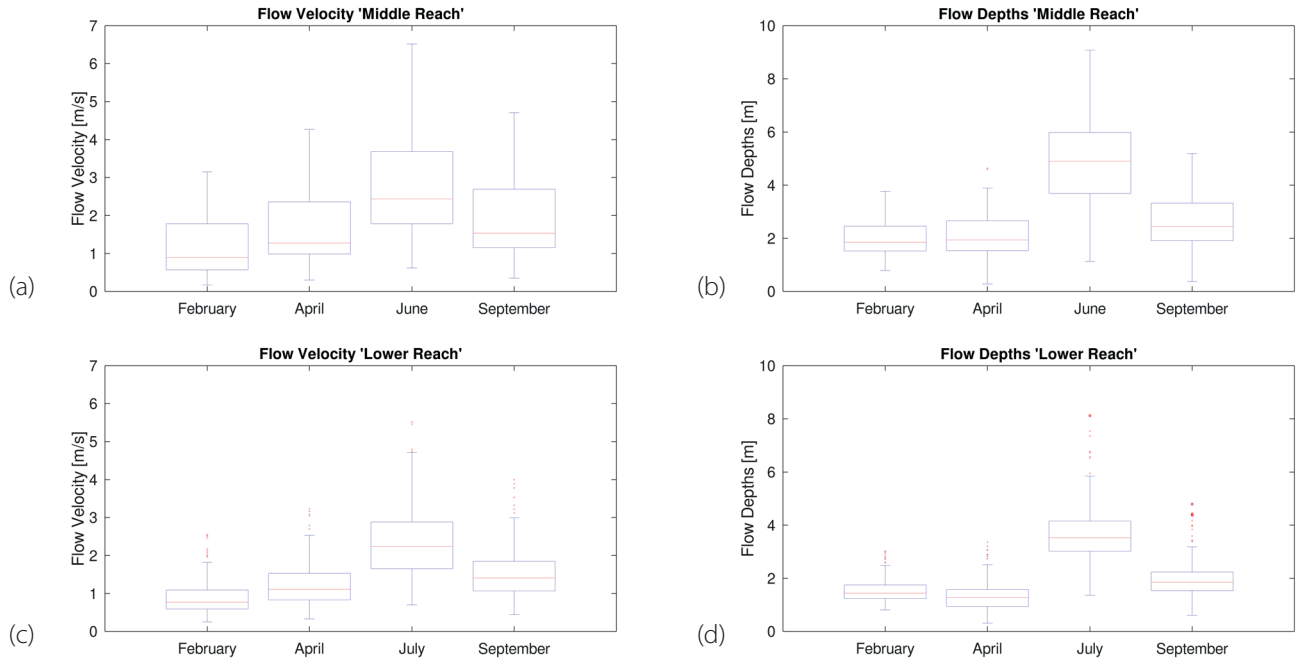

Fig. 9. Annual variability of flow velocities and corresponding flow are based on one-dimensional flow simulation in HEC-Ras – a) flow velocities middle reach b) flow depths middle reach c) flow velocities lower reach d) flow depths lower reach

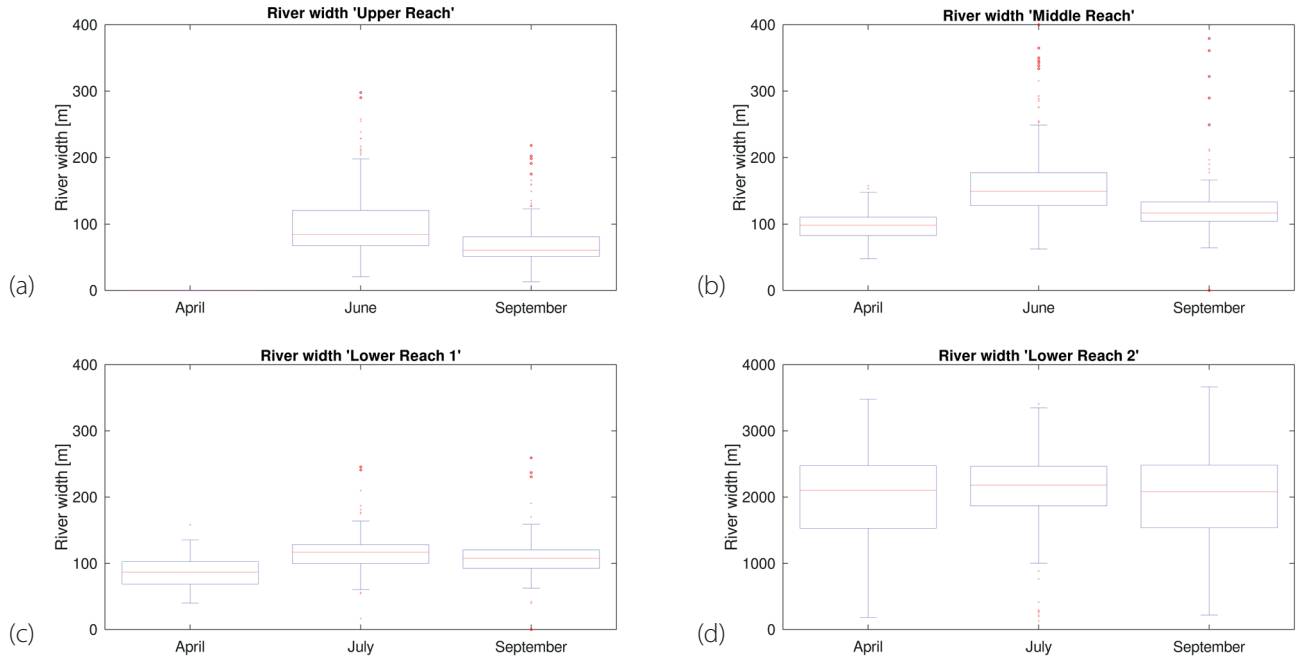

Fig. 10. Annual river width variability in the upper, middle and lower reaches of the Katun– a) River width upper reach b) River width middle reach c) River width lower reach 1 d) River width lower reach 2

to the GIS-based approach and missing data regarding riparian vegetation no statement can be made about the quality of the exchange with the floodplain areas, since more detailed models than the one used in this paper are needed for this (Maharjan and Shakya 2016).

When analysing the sinuosity of the river Katun using the simplified formula for three different section lengths along the entire Katun, the results suggest the use of 1 km for section length. For this length the calculations provide the lowest standard deviation and thus the most consistent results (Table 5).

The high difference between the two DEMs under consideration is probably due to the different resolution. Because of the resolution, the maximum values for the two years should also be viewed with caution. Both the 1.5 and 1.7 represent outliers and are at locations where the river axis does not clearly coincide with satellite data from those years. Nevertheless, such high values indicate stretches of the Katun River that can be described as strongly meandering and occur more frequently, especially in the middle and lower reaches. Based on the following, more detailed calculations of the SSI in each of the selected section the entire Katun can be described as straight to slightly sinusoidal based on Table 6. According to the different hydromorphology in the lower reaches, a determination of SSI should have been carried out for two different locations. Due to difficulties with the determination of a main river axis sole based on GIS data this was not performed.

Table 5. Results of the simplified sinuosity calculations

SRTM GLOBAL	1 km	5 km	10 km		GMTED2010	1 km	5 km	10 km
Mean	1.10	1.23	1.29		Mean	1.06	1.17	1.06
Std	0.09	0.15	0.20		Std	0.08	0.13	0
Max	1.76	1.69	2.09		Max	1.57	1.91	1.06

Table 6. Muellers sinuosity index for channel lengths of 5, 25 and 50 km in the upper, middle and lower reaches of the Katun

SSI	CL = 50 km	CL = 25 km	CL = 5 km
Upper Reach	1.02	1.03	1.09
Middle Reach	1.05	1.04	1.14
Lower Reach	0.99	1.0	0.97

Table 7. Hydromorphological characterisation of the Katun River

	Upper reach	Middle reach	Lower reach
River kilometer [km]	1 - 210	211 - 410	411 - 688
Flow order number	5	6 - 7	7
Sinuosity SSI [-]	1.03	1.04	1.00
River width [m]	65 - 110	97 - 165	86 - 108 1,975 – 2,025
Bottom slope [%]	0.41	0.19	0.14
D50 on the banks [mm]	-	52 - 77	18 - 32
Manning value n (banks) [s/m1/3]	-	0.066 – 0.07	0.055 – 0.061
Strickler value kSt (bank) [m/s1/3]	-	14.3 – 15.2	16.4 – 18.1
Gauge (Catchment in km^2)	Tyungur (13,415) *	Maly Yaloman (36,608)	Srostky (58,113)
Discharge MQ (min - max) [m^3/s]	266 (44 - 832)	466 (85 - 1.488)	614 (87 - 1.743)
Specific discharge MQ (min - max) [L/s/km^2]	19.83 (3.28 – 62.02)	12.73 (2.32 – 40.65)	10.57 (1.49 – 29.99)
Flow velocity v [m/s]	-	1.16 – 2.74	0.92 – 2.36
Maximum flow depth [m]	-	1.97 – 4.88	1.54 – 3.63
Shear stresses [N/m^2]	-	20.63 – 100.48	9.44 – 55.64
Flow energy [N/ms]	-	41.66 – 404.30	14.04 – 178.68
Dominant vegetation type of the riparian strips		Grasses / Shrubs	Saplings and trees
Vegetation structure of the riparian strips	-	simple	complex
* = Geographical location of the Tyungur gauge in the middle reaches. However, since it is located upstream of the confluence with the Argut and the Chuya, it is cited as a reference for the discharge of the upper reach.			

CONCLUSIONS

Our case study from Katun River underlines the importance of longitudinal (connectivity), lateral (floodplains), vertical (sediments) and temporal (annual variability of flow) aspects, which are the 4-dimensions of a lotic ecosystem (Ward 1989). Based on our investigations of large-scale hydromorphological characteristics along the Katun, guiding principles for glacier rivers were developed (Table 7). As shown for the individual parameters (e.g. slope, width, etc.), they influence each other and are strongly dependent as well as characteristic for each river section. In the context of revitalisation of straightened and / or channelized river courses, it is important to focus on the processes of this interaction and provide suitable space for lateral expansion. The aim of revitalisation measures should be to enable the river to support its natural dynamics and after an initial situation is created the river should form the newly gained riverscape itself.

In most rivers, which were altered by human activities, the longitudinal continuity is limited, both for fish and sediments. Straightened rivers deepen over time, which causes the adjacent riparian strips and floodplains to dry out, as the river no longer spills out during floods. The surveys along Katun river showed a diverse and structured riparian vegetation, which forms an important habitat and migration corridor (Peredo Arce et al. 2021). Therefore, another essential aspect is recommended re-establish habitats where the development of typical riparian vegetation is enabled. This can be either achieved (i) by lowering the floodplains to enable periodical flooding of the riparian vegetation or (ii) by widening the river which decreases the shear stress, leading to a rising river bed and better connected floodplains due to newly created sedimentation.

REFERENCES

Allan J., Castillo M. (2007). Stream ecology. Structure and function of running waters. 2nd ed, reprinted. Dordrecht: Springer.

Allen G., Pavelsky T. (2018). Global extent of rivers and streams. In: Science (New York, N.Y.), 361 (6402), 585-588, DOI: 10.1126/science.aat0636.

Arcement G., Schneider V. (1989) Guide for Selecting Manning's Roughness Coefficients for Natural Channels and Flood Plains. U.S. Geological Survey Water-supply Paper: U.S. Government Printing Office.

Baeyens W., Dehandschutter B., Leermakers M., Bobrov V., Hus R., Baeyens-Volant D. (2003). Natural Mercury Levels in Geologically Enriched and Geologically Active Areas. Case Study of Katun River and Lake Teletskoye, Altai (Siberia). In: Water, Air, and Soil Pollution, 142 (1/4), 375-393, DOI: 10.1023/A:1022099410739.

Belletti B., Rinaldi M., Buijse A., Gurnell A., Mosselman E. (2015). A review of assessment methods for river hydromorphology. In: Environ Earth Sci, 73 (5), 2079–2100, DOI: 10.1007/s12665-014-3558-1.

Brunner G. (2016). HEC-RAS River Analysis System. Hydraulic Reference Manual Version 5.0. Davis, CA: US Army Corps of Engineers, Hydrologic Engineering Center, [online] Available at: https://www.hec.usace.army.mil/software/hec-ras/documentation/HEC-RAS%205.0%20Reference%20Manual.pdf [Accessed 14 Mar. 2020].

Revyakin V. (1978). Catalog of glaciers of the USSR. Altai and West Siberia. 1978. v.15, issue 1. Gidrometeoizdat (in Russian).

Chow V. (1959). Open-Channel Hydraulics. New York: McGraw-Hill Book Company.

Díaz-Redondo M., Egger G., Marchamalo M., Damm C., Oliveira R., Schmitt L. (2018). Targeting lateral connectivity and morphodynamics in a large river-floodplain system: The upper Rhine River. In: River Res Applic, 34 (7), 734-744, DOI: 10.1002/rra.3287.

Dai C., Durand M., Howat I.M., Altenau E.H., Pavelsky T.M. 2018. Estimating River Surface Eleva-tion From ArcticDEM. Geophysical Research Letters, 45, 3107–3114, DOI: 10.1002/2018GL077379.

Du Y., Zhang Y., Ling F., Wang Q., Li W., Li X. (2016). Water Bodies' Mapping from Sentinel-2 Imagery with Modified Normalized Difference Water Index at 10-m Spatial Resolution Produced by Sharpening the SWIR Band. In: Remote Sensing, 8 (4), 354, DOI: 10.3390/rs8040354.

Environment Agency (2003). River habitat survey in Britain and Ireland. Field survey guidance manual. Bristol: Environment Agency.

FOEN (2013). Fliessgewässertypisierung der Schweiz. A basis for watercourse assessment and development. Annex 5. ed. by Federal Office for the Environment FOEN. Bern, [online] Available at: https://www.bafu.admin.ch/bafu/de/home/themen/wasser/publikationen-studien/publikationen-wasser/fliessgewaessertypisierung-der-schweiz.html [Accessed 09 Apr 2020].

Galia T., Škarpich V., Gajdošová K., Krpec P. (2017). Variability Of Wolman Pebble Samples in Gravel/Cobble Bed Streams. In: ASP FC, 1, 237-246, DOI: 10.15576/ASP.FC/2017.16.1.237.

Haggett P., Chorley R. (1969). Network analysis in geography. London: Edward Arnold.

Haywood A. (2010). Siberia. A cultural history (Landscapes of the Imagination). Oxford, New York: Oxford University Press.

Huet M. (1949). Aperçu des relations entre la pente et les populations piscicoles des eaux courantes. In: Swiss Journal of Hydrology, 11, 332-351, DOI: 10.1007/BF02503356.

Iturrizaga, L. (2011). Glacier Lake Outburst Floods. In: Singh, V.P., Singh, P., Haritashya, U.K. (eds) Encyclopedia of Snow, Ice and Glaciers. Encyclopedia of Earth Sciences Series. Springer, Dordrecht, 381-399, DOI: 10.1007/978-90-481-2642-2_196.

Khan A., Rao L., Yunus A., Govil H. (2018). Characterization of channel planform features and sinuosity indices in parts of Yamuna River flood plain using remote sensing and GIS techniques. In: Arab J Geosci, 11 (17), 263, DOI: 10.1007/s12517-018-3876-9.

Khromova T., Nosenko G., Glazovsky A., Muraviev A., Nikitin S., Lavrentiev I. (2021). New Inventory of the Russian glaciers based on satellite data (2016–2019). In: Ice and Snow, 61 (3), 341–358 (in Russian), DOI: 10.31857/S2076673421030093.

Kirpotin, S., Nemceva, G. (2015) Environmental, economic and social risks of nuclear power engineering (the case of the southern part of the Ob-river basin). In: International Journal of Environmental Studies, 72 (3), 580-591, DOI: 10.1080/00207233.2015.1027589.

Lammers, R., Shiklomanov, A., Vörösmarty C., Fekete B., Peterson B. (2016). R-ArcticNet, A Regional Hydrographic Data Network for the Pan-Arctic Region. supplement to: Lammers, Richard B, Shiklomanov, Alexander I, Vörösmarty, Charles J, Fekete, Balázs M, Peterson, Bruce J (2001). Assessment of contemporary Arctic river runoff based on observational discharge records. Journal of Geophysical Research: Atmospheres, [online] Available at: http://www.r-arcticnet.sr.unh.edu/v4.0/index.html [Accessed 27 Mar. 2020].

Leopold L., Miller J. (1956). Ephemeral streams - Hydraulic factors and their relation to the drainage net. With the cooperation of U.S. Government Printing Office. Washington, DC. (Professional Paper, 282A), [online] Available at: http://pubs.er.usgs.gov/publication/pp282A [Accessed 17 Feb. 2020].

Maharjan L., Shakya N. (2016). Comparative Study of One Dimensional and Two Dimensional Steady Surface Flow Analysis. Journal of Advanced College of Engineering and Management, 2, 15-30, DOI: 10.3126/jacem.v2i0.16095.

Mandych A. (2006). Conditions and Trends in Natural Systems of the Altai-Sayan Ecoregion. In: Hartmut Vogtmann and Nikolai Dobretsov (eds.). Environmental Security and Sustainable Land Use - with special reference to Central Asia, vol. 5, Dordrecht: Kluwer Academic Publishers (NATO Security through Science Series), 231-275.

Mueller J. (1968). An Introduction to the Hydraulic and Topographic Sinuosity Indexes. Annals of the Association of American Geographers, 58 (2), 371-385. DOI:10.1111/j.1467-8306.1968.tb00650.x.

Newson M., Large A. (2006). 'Natural' rivers, 'hydromorphological quality' and river restoration: a challenging new agenda for applied fluvial geo-morphology. In: Earth Surf. Process. Landforms, 31 (13), 1606–1624, DOI: 10.1002/esp.1430.

Nikora V., Goring D., Biggs B. (1998). On gravel-bed roughness characterization. In: Water Resources Research, 34 (3), 517-527, DOI: 10.1029/97WR02886.

Peredo Arce A., Hörren T., Schletterer M., Kail J. (2021). How far can EPTs fly? A comparison of empirical flying distances of riverine invertebrates and existing dispersal metrics. Ecological Indicators, 125, 107-465, DOI: 10.1016/j.ecolind.2021.107465.

Purinton B, Bookhagen B. (2017). Validation of digital elevation models (DEMs) and comparison of geomorphic metrics on the southern Central Andean Plateau. Earth Surface Dynamics, 5, 211–237, DOI: 10.5194/esurf-5-211-2017.

Sapozhnikov V. (1949). On the Russian and Mongolian Altai, 198 (in Russian).

Schletterer M., Shevchenko A., Yanygina L., Manakov Y., Reisenbüchler M., Rutschmann P. (2021a). Eindrücke vom Oberlauf des Obs in Russland. WASSERWIRTSCHAFT, 111, 77-85, DOI: 10.1007/s35147-021-0903-7.

Schletterer M., Reisenbüchler M., Berg L., Zunic F., Rutschmann P. (2021b). Reisebericht zur Wasserbauexkursion 2019 der TU München nach Sibirien. WASSERWIRTSCHAFT, 111, 96-101, DOI: 10.1007/s35147-021-0902-8.

Schmalfuß L., Hauer C., Yanygina L. V., Schletterer M. (2022). Landscape Reading for Alpine Rivers: A Case Study from the river Biya. Geography, Environment, Sustainability, 4(15), 196-213, DOI: 10.24057/2071-9388-2022-046

Schumm S. (1977). The fluvial system. New York: Wiley (A Wiley-Interscience publication).

Shiklomanov A., Lammers R. (2014). River ice responses to a warming Arctic - recent evidence from Russian rivers. In: Environ. Res. Lett., 9 (3), 35008, DOI: 10.1088/1748-9326/9/3/035008.

Shiklomanov A., Yakovleva T., Lammers R., Karasev I., Vörösmarty C., Linder E. (2006). Cold region river discharge uncertainty – estimates from large Russian rivers. Journal of Hydrology, 326 (1–4), 231-256. DOI: 10.1016/j.jhydrol.2005.10.037.

Strahler A. (1957). Quantitative analysis of watershed geomorphology. In: American Geophysical Union Transaction, 38 (6), 913-920.

Vuglinsky V., Valatin D. (2018). Changes in Ice Cover Duration and Maximum Ice Thickness for Rivers and Lakes in the Asian Part of Russia. In: NR 09 (03), 73-87, DOI: 10.4236/nr.2018.93006.

Ward J. (1989). The four-dimensional nature of lotic ecosystems. J N Am Benthol Soc, 8, 2–8, DOI: 10.2307/1467397

Wolman G. (1954). A Method of Sampling River-Bed Material. In: Transactions, American Geophysical Union, 35 (6), 951-956.

Zerbe S. (2019). Renaturierung von Ökosystemen im Spannungsfeld von Mensch und Umwelt. An interdisciplinary textbook. 1st ed. 2019, DOI: 10.1007/978-3-662-58650-1.

Zhang D., Yang Y., Lan B. (2018). Climate variability in the northern and southern Altai Mountains during the past 50 years. In: Scientific reports, 8 (1), 32-38, DOI: 10.1038/s41598-018-21637-x.